Electronic orders in the Verwey structure of magnetite

Electronic orders in the Verwey structure of magnetite

Mark S. Senn,[1] Ingo Loa,[2] Jon P. Wright,[3] and J. Paul Attfield[1,*]

[1]*Centre for Science at Extreme Conditions and School of Chemistry, University of Edinburgh, West Mains Road, Edinburgh, EH9 3JZ, United Kingdom*

[2]*SUPA, Centre for Science at Extreme Conditions and School of Physics and Astronomy, University of Edinburgh, Mayfield Road, Edinburgh, EH9 3JZ, United Kingdom*

[3]*European Synchrotron Radiation Facility, 6 rue Jules Horowitz, Grenoble Cedex 9, 38000 France*

(Received 28 February 2012; published 21 March 2012)

Electronic structure calculations of the Verwey ground state of magnetite, Fe_3O_4, using density functional theory with treatment of on-site Coulomb interactions (DFT + U scheme), are reported. These calculations use the recently published experimental crystal structure coordinates for magnetite in the monoclinic space group Cc. The computed density distribution for minority spin electron states close to the Fermi level demonstrates that charge order and Fe^{2+}-orbital order are present at the B-type lattice sites to a first approximation. However, Fe^{2+}/Fe^{3+} charge differences are diminished through weak bonding interactions of the Fe^{2+} states to specific pairs of neighboring iron sites that create linear, three-B-atom trimeron units that may be regarded as orbital molecules. Trimerons are ordered evenly along most Fe atom chains in the Verwey structure, but more complex interactions are observed within one chain.

DOI: 10.1103/PhysRevB.85.125119 PACS number(s): 71.30.+h, 71.20.Ps, 75.25.Dk, 75.47.Lx

I. INTRODUCTION

Magnetite (Fe_3O_4) is the eponymous magnetic substance and occurs widely on earth as a mineral and biomineral. In this AB_2O_4 spinel-type material, there are twice as many B-site Fe^{3+} $3d^5$ $S = 5/2$ up-spins as there are down-spins at the A sites, resulting in a net magnetization. Rapid hopping of an extra down-spin electron between B sites, as represented in the formal charge distribution $Fe^{3+}[Fe^{2.5+}]_2O_4$, results in minority-spin-polarized electronic conductivity. On cooling, a sharp first-order transition is observed in measurements of heat capacity, conductivity, magnetization, and many other properties at around 125 K.[1,2] This is accompanied by a complex lattice distortion to a monoclinic $\sqrt{2} \times \sqrt{2} \times 2$ superstructure of the cubic room temperature lattice.[3,4] The supercell has Cc space group symmetry and contains 224 atoms. Verwey proposed that the transition is driven by a regular condensation of Fe^{2+} and Fe^{3+} ions equivalent to localization of the minority spin extra electrons,[1] a phenomenon now known as charge ordering that has been verified in many other oxides.[5] However, the ground state of magnetite has remained a contentious issue for over 70 years, as microtwinning of Cc domains below the Verwey transition hampers diffraction studies of the low-temperature structure. Partial structure refinements from powder diffraction data[6–8] and resonant x-ray studies[9–13] have led to a variety of proposed charge-ordered and bond-dimerized ground state models in recent years.[14–20]

An x-ray refinement of the full low-temperature Cc superstructure of magnetite was recently reported.[21] A large number of frozen phonon modes were found to contribute to the overall structural distortion. Fe^{2+}/Fe^{3+} charge ordering and Fe^{2+} orbital ordering was proposed from analysis of the observed interatomic distances, showing that Verwey's hypothesis[1] is correct to a useful first approximation. The observed charge ordering pattern is consistent with predictions of two recent electronic band structure calculations based on density functional theory (DFT) with treatment of on-site Coulomb interactions (DFT + U scheme),[16,18] and the observed orbital order was also predicted in Ref. 18. However, additional structural distortions in which B-site Fe-Fe distances within linear Fe-Fe-Fe units are anomalously shortened suggested that the extra down-spin electrons are not fully localized as Fe^{2+} states, but are instead spread over three sites resulting in highly structured three-site polarons termed trimerons. Some Fe^{3+} displacements consistent with trimeron formation were noted in Ref. 18, but the bond-dimerization scheme presented in Ref. 20 is not supported by the experimental structure, and trimeron order was not proposed in previous studies. Here, we report electronic structure calculations for the experimental Cc structural model, which provide further insights into the charge, orbital, and trimeron orders in magnetite.

II. ELECTRONIC STRUCTURE CALCULATIONS

Electronic structure calculations were performed in the framework of density functional theory with the full-potential augmented plane-wave plus local orbital method as implemented in the WIEN2K code.[22] The spin-polarized calculations were performed for the full Cc crystal structure with 112 atoms in the primitive unit cell, using the lattice parameters and atomic positions determined recently at 90 K.[21] The $3s$, $3p$, $3d$, and $4s$ orbitals of Fe and the $2s$ and $2p$ orbitals of O were treated as valence states, and additional local orbitals were used for Fe s and p states and O s states. Electron exchange and correlation were considered in the generalized gradient approximation (GGA)[23] with additional treatment of on-site Coulomb repulsion using the DFT + U approach.[24] An on-site Coulomb energy of $U = 4.5$ eV and an exchange parameter $J = 0.9$ eV were used for all Fe d states as in previous work.[15,16,18] Brillouin zone integration was performed on a regular mesh of $6 \times 6 \times 2$ k points with 21 k points in the irreducible part of the Brillouin zone. Atomic sphere muffin tin radii (R_{MT}) of 1.86 bohr and 1.65 bohr were chosen for Fe and O, respectively, and the largest plane-wave vector K_{max} was given by $R_{MT}K_{max} = 8$. Spin-orbit coupling was not considered.

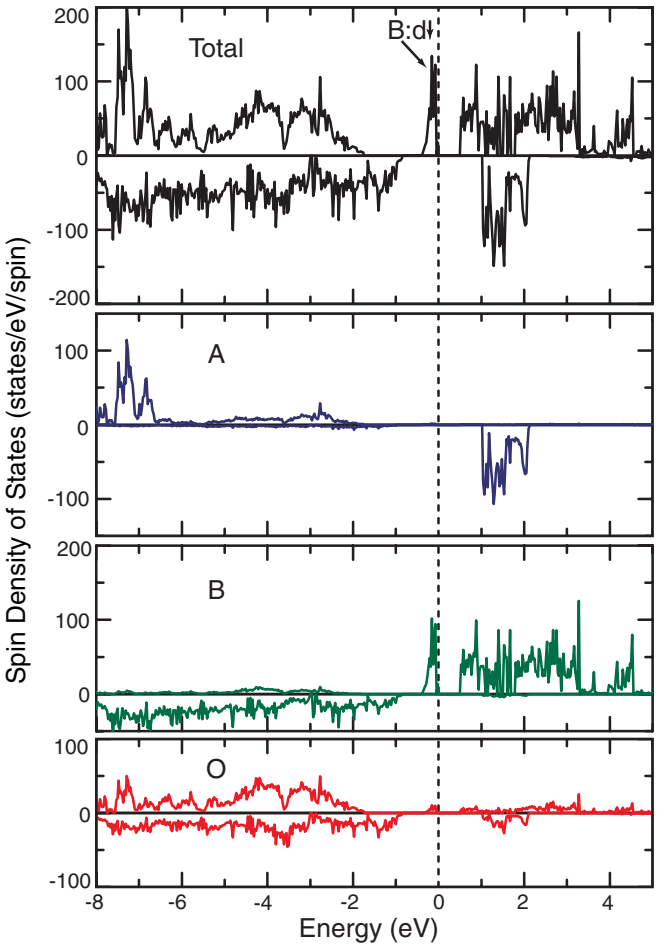

FIG. 1. (Color online) Spin-dependent electronic density of states for the Cc Verwey structure of magnetite calculated from experimental structural parameters in Ref. 21. Energies are shown relative to the Fermi level, which lies at the top of the B:$d\downarrow$ band. Contributions from the A (tetrahedrally coordinated Fe), B (octahedrally coordinated Fe), and O atoms are shown below the total density. Upper/lower sections correspond to minority (down)/majority (up) spin states in all plots.

The calculated electronic density of states for magnetite around the Fermi energy is shown in Fig. 1. Gaps in both the spin-up and spin-down channels are observed, consistent with the insulating nature of the Verwey phase, and the estimated band gap in the down-spin states is 500 meV, which is somewhat larger than experimental values of ∼100 meV from spectroscopic measurements.[25] The narrow down-spin band just below the Fermi level consists almost entirely of B-atom d states corresponding to the extra electrons. The spatial distribution of this electron density is of particular interest in relation to the Verwey distortion, and we refer to the states at energies between -460 and 0 meV as the B:$d\downarrow$ band hereafter. Below another 435-meV gap lie broad bands corresponding to the A site (down-spin) and B site (up-spin) Fe^{3+} $3d^5$ states, plus oxygen $2s$ and $2p$ contributions.

III. ELECTRONIC ORDERS

To verify the charge ordering deduced from analysis of Fe-O distances in Ref. 21, both the total charge density and the B:$d\downarrow$ band densities were integrated within the Fe atomic spheres. These are plotted against the structural bond valence sum (BVS) estimates of formal Fe charge for the 16 symmetry-independent B sites in the Cc magnetite structure in Fig. 2. Both integrated charges correlate with the BVS estimates, as the Fe^{2+}-like sites with the lowest eight BVS values have the highest eight integrated charges and vice versa for the Fe^{3+}-like sites. The B:$d\downarrow$ charges cover a range of $0.33e$ (where e is the electron charge), but the range in total charge is smaller ($0.15e$), showing that redistribution of charge from the majority spin B:d and oxygen $2s$ and $2p$ bands tends to smear out the charge differences. Neither the integrated charges nor the BVS distributions have the bimodal character expected for an ideal Fe^{2+}/Fe^{3+} charge ordering, and this evidences the charge redistribution within trimerons (inset of Fig. 2) discussed later.

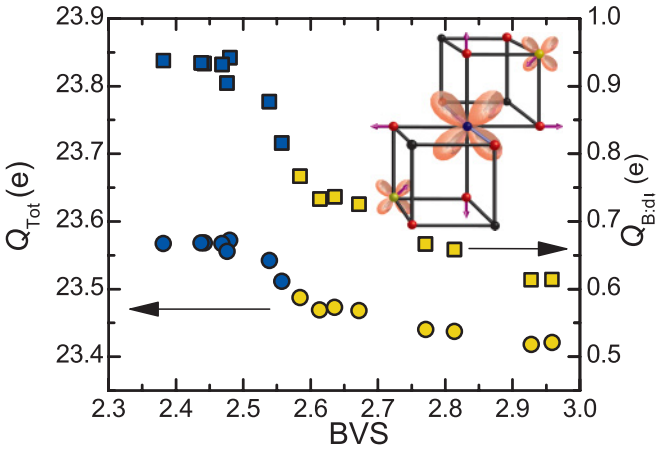

FIG. 2. (Color online) Integrated total charges Q_{Tot} and charges from the B:$d\downarrow$ band $Q_{B:d\downarrow}$ for the 16 independent B iron sites in the Cc magnetite structure, plotted against the structural bond valence sum (BVS) estimates of formal charge state in Ref. 21. Symbols with dark/light fill correspond to the identified Fe^{2+}/Fe^{3+}-like states. Inset shows the idealized local structure of a trimeron. A minority spin d electron is localized at one of the t_{2g} orbitals on the central B atom (an Fe^{2+} state). This orbital order elongates the four Fe-O bonds in the plane of the occupied t_{2g} orbital, and weak bonding interactions transfer electron density into coplanar t_{2g} orbitals at two of the six neighboring B sites, which tends to contract the distances to these two atoms and diminishes the charge difference between Fe^{2+}- and Fe^{3+}- like states.

Orbital ordering in the Cc magnetite structure is apparent from the electron density isosurface[26] for the B:$d\downarrow$ band states shown in Fig. 3. The narrowness of the band is reflected in the atomic $3d$-orbital-like nature of the densities at the B sites. Here, B:$d\downarrow$ density with t_{2g} symmetry in the axis system of the local BO_6 octahedra is observed at each Fe^{2+} site, demonstrating that a well-defined orbital order is present.[18] Significant B:$d\downarrow$ density is also apparent at the six Fe^{3+}-like sites that participate in trimeron bonding with the Fe^{2+} sites, and this shows various $3d$-orbital symmetries according to the number of trimerons (from one to three) terminating at the site. The two Fe^{3+}-like sites that do not participate in trimerons have the lowest integrated charges and highest BVSs in Fig. 2 and are the two atoms that show very small B:$d\downarrow$ isosurfaces in Fig. 3, confirming that they are the closest to ideal Fe^{3+} states. The observation of anomalously short Fe^{2+}-Fe^{3+} distances

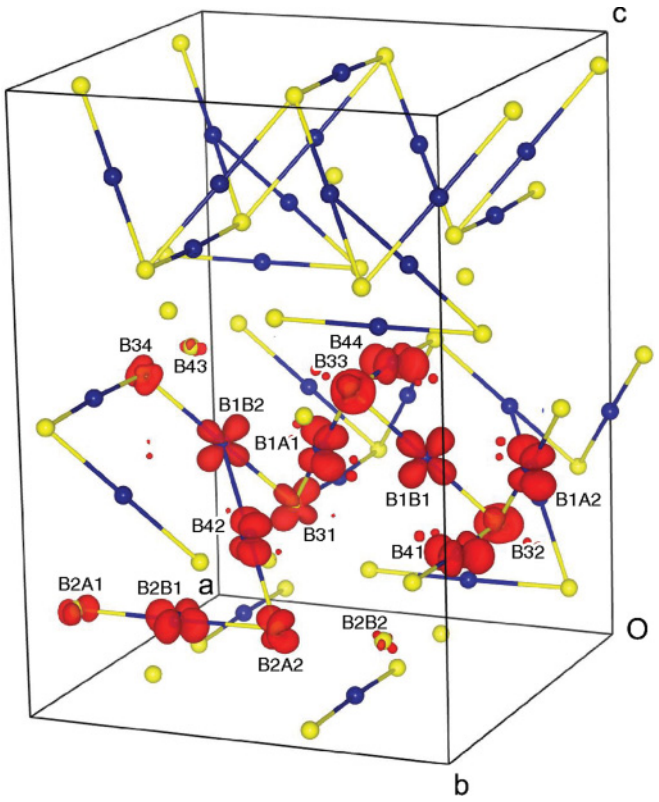

FIG. 3. (Color online) The Cc unit cell of magnetite with B site Fe^{2+}/Fe^{3+}-like states drawn as dark/light spheres and trimeron connections between B sites shown as proposed in Ref. 21. The isosurface for the B:$d\downarrow$ band states at an electron density of 0.1 e/Å^3 is shown in the lower part of the unit cell for the 16 independent B sites, labeled as in Ref. 21.

perpendicular to the local orbital order axes at Fe^{2+} sites in the 90 K Cc magnetite structure[21] was taken as evidence for the formation of linear trimeron units of three coupled B sites in which a minority-spin t_{2g} electron is delocalized from a central Fe^{2+} ion onto two neighbors, resulting in weak bonding interactions (see Fig. 2 inset). This is supported by the substantial B:$d\downarrow$ density observed at the Fe^{3+}-like sites that participate in trimerons in Fig. 3.

The ~3 Å B-B connections comprise infinite linear chains parallel to six directions in the magnetite structure. Each B site lies at the intersection of three chains. The B:$d\downarrow$ electron density variations in the repeat sequences for all distinct chains are shown in Fig. 4(a). Enhanced electron densities at the trimeron termini are observed, consistent with the trimeron model in the inset to Fig. 2, where B:$d\downarrow$ electron density is transferred from the central Fe^{2+} ion to the two terminal neighbors. This is quantified using values of the B:$d\downarrow$ electron density maxima at the lobes lying ~0.3 Å on both sides of the nucleus in the chain directions. The average B:$d\downarrow$ electron density at the maxima of the eight Fe^{2+} trimeron centers in Fig. 4(a) (between the two T symbols) is 3.47 eÅ^{-3}. This high value is in keeping with the orbital order in these directions. The corresponding average for the 16 terminal trimeron lobes (15 of which are from Fe^{3+}-type sites) is 0.45 eÅ^{-3}, whereas the average for the 24 other lobes (from 15 Fe^{2+}-like and 9 Fe^{3+}-like sites, traversed in nontrimeron directions) is 0.07 eÅ^{-3}. The disparity between the latter two averages would

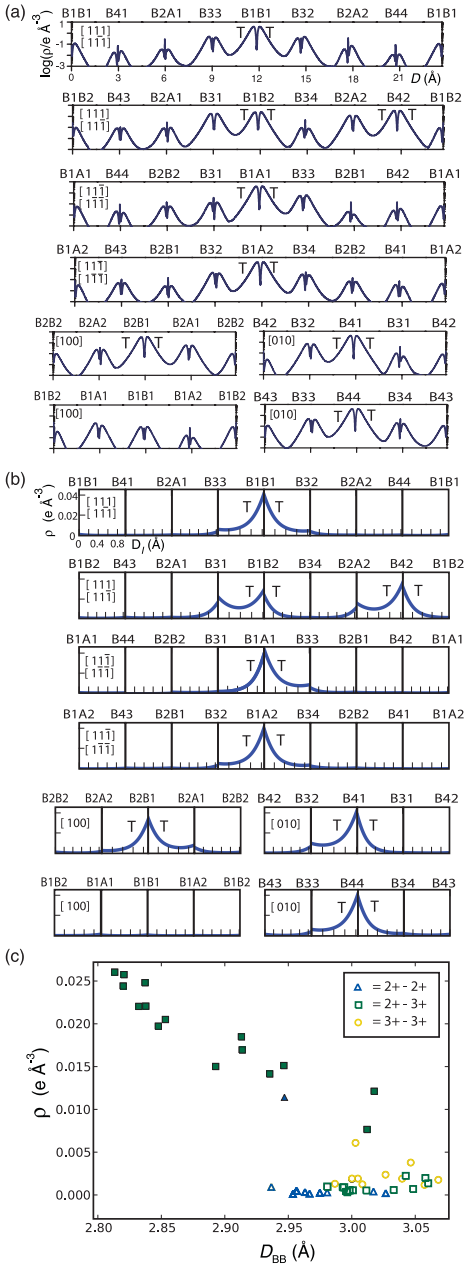

FIG. 4. (Color online) Plots of calculated B:$d\downarrow$ electron density (ρ) for Fe atoms in the Cc magnetite structure. (a) and (b) display variations in ρ along the B-B vectors for all of the independent linear B chain repeat sequences, with their lattice directions shown. B-site labels are the same as in Fig. 3 and Ref. 21 and show how the sites are related to those in an earlier $P2/c$ subcell model (Ref. 7). The eight consecutive B-B pairs assigned to trimerons are indicated by T symbols. (a) B:$d\downarrow$ density variations for $\rho > 10^{-3}$ eÅ^{-3} on a log scale plotted against cumulative B-to-B chain distance D. All plots have the same scales. (b) ρ variations in the central sections between neighboring B-site Fe atoms. Each central distance scale D_I is along the straight line within a B-B pair, starting 1 Å from the first atom center and ending 1 Å from the second. All plots use the same scales. (c) Plot of the average central section electron densities from the 48 panels in (b) against the B-B distances. The symbols show the idealized charge states for the two B sites, and closed/open symbols indicate expected trimeron/nontrimeron B-B pairs.

not be expected in a simple charge and orbital ordered model and evidences the charge transfer within trimerons that smears out the first approximation Fe^{2+}/Fe^{3+}charge order.

Charge transfer also results in a relatively large $B{:}d\downarrow$ electron density throughout the line connecting the three B sites in each trimeron. This is seen by plotting the $B{:}d\downarrow$ electron density variations along the central sections (∼1 Å in extent) of the straight lines connecting nearest neighbor pairs of B sites, outside the R_{MT} radii of the two Fe atoms. Near-symmetric pairs of high $B{:}d\downarrow$ density central sections are observed for most of the predicted B-B trimeron pairs in Fig. 4(b), and very low density is observed elsewhere. However, a more complex electron localization is observed along one of the [111] chains [second row in Figs. 4(a) and 4(b)] as discussed below. These trimeron orderings are equivalent to static charge density waves of four- or eight-B-atom periodicities in the various chain directions.

B-site chains parallel to the [100] and [010] directions have four-atom repeat sequences. One [100] chain [consisting of $B1$ sites derived from the $B1$ position in the previously reported $P2/c$ subcell;[7] shown lowest left in Figs. 4(a) and 4(b)] is unique to the entire low-temperature magnetite structure as it contains no trimerons. As noted in Ref. 21, this is the only chain to contain only Fe^{2+}-like states; however, orbital ordering results in all their trimerons being directed along other chain directions. B-site chains in the ⟨111⟩-type directions have repeat sequences of eight atoms. Each chain intersects a symmetry-generated equivalent of itself at just one $B1$-type site (e.g. the top panels of Figs. 4(a) and 4(b) show that equivalent chains parallel to [111] and $[1\bar{1}1]$ intersect only at $B1B1$ sites) where trimerons are centered in all four cases. One of these chains contains an additional trimeron [the $B42$ site in the second row in Figs. 4(a) and 4(b)], making this the only chain in which unequal three- and five-atom trimeron spacings occur. This perturbs the $B{:}d\downarrow$ density, especially for the $B1B2$ trimeron, where the central section density is spread almost symmetrically over four successive B atoms. This could be viewed as a bond-dimer localized charge, spread over the adjacent two neighbors in the chain, but no other evidence for bond-dimer order is observed in the Cc structure, and the central section $B{:}d\downarrow$ densities are consistent with trimeron order in all other cases.

The 16 B-B contacts identified as being within trimerons are seen to be those with the highest average $B{:}d\downarrow$ central section densities in Fig. 4(c). Although 14 of these B-B distances are short, high $B{:}d\downarrow$ density is also observed in the central sections of the two long predicted trimeron B-B distances, demonstrating that $B{:}d\downarrow$ electron density is not a simple function of B-B distance. The lowest trimeron and highest nontrimeron $B{:}d\downarrow$ density value points, which are proximate at $D_{BB} = 3.012$ and 3.003 Å on Fig. 4(c), correspond to the two outer B-B distances in the four-atom $B1B2$ $B{:}d\downarrow$ distribution noted above, which represents the greatest perturbation of the trimeron order.

The trimerons observed in the low-temperature magnetite structure may be regarded as orbital molecules — locally coupled orbital states on two or more metal ions within an orbitally ordered solid. The magnetite trimerons are one-electron quasiparticles with effective spin-1/2. Previously reported species that may be classified as orbital molecules are polyelectronic spin-singlet species, usually two-electron dimers, e.g. in $CuIr_2S_4$ (Ref. 27) and $MgTi_2O_4$ (Ref. 28), which can show remarkable arrangements such as the spontaneous chirality of helical structures in $MgTi_2O_4$. However, more complex species like heptameric, 18-electron, spin-singlet $V_7{}^{17+}$ clusters in AlV_2O_4 have also been reported.[29] Taken together, these reports demonstrate that orbital molecules may be identified as a class of quantum electronic states formed through orbital order in structures such as spinel, where direct metal-metal interactions are significant. The structure of the Verwey phase of magnetite demonstrates that complex electronic orders can emerge from the self-organization of orbital molecules in solids, analogous to the formation of complex molecules from atoms in conventional matter.

IV. CONCLUSIONS

In conclusion, we have performed DFT + U calculations of the electronic structure of magnetite using the low-temperature Cc structure recently determined by x-ray crystallography.[21] A band gap of ∼0.5 eV is calculated. The narrow minority spin band just below the Fermi level consisting predominantly of B-atom d states is of particular interest as it describes the extra electrons that were predicted to be localized by Verwey[1] and subsequent authors. The spatial distribution of this $B{:}d\downarrow$ electron density is consistent with charge ordering and a well-defined orbital ordering at the Fe^{2+}-like sites. However, significant transfer of $B{:}d\downarrow$ density to most of the Fe^{3+}-like sites is also observed, and the variations in $B{:}d\downarrow$ density between neighboring B-B pairs supports a trimeron ordering description in which extra electrons are localized within linear three-B-atom units. The trimeron units are evenly distributed along most of the infinite B-site chains, but an irregular spacing distorts the $B{:}d\downarrow$ distribution in one case. Hence, the overall electronic order in the Verwey structure approximates to a Fe^{2+}/Fe^{3+} charge and orbital model but with significant discrepancies that are usefully described as trimeron order. Trimerons are one of several known examples of orbital molecules which can self-organize to generate complex electronic arrangements in orbitally ordered solids.

ACKNOWLEDGMENTS

We acknowledge support from EPSRC, STFC, and the Leverhulme Trust. This work used resources provided by the Edinburgh Compute and Data Facility (ECDF, www.ecdf.ed.ac.uk); the ECDF is partially supported by the eDIKT initiative (www.edikt.org.uk).

*j.p.attfield@ed.ac.uk

[1] E. J. W. Verwey, Nature (London) **144**, 327 (1939).
[2] F. Walz, J. Phys. Condens. Matter **14**, R285 (2002).
[3] J. Yoshida and S. Iida, J. Phys. Soc. Jpn. **42**, 230 (1977).
[4] M. Iizumi, T. F. Koetzle, G. Shirane, S. Chikazumi, M. Matsui, and S. Todo, Acta Crystallogr. B **38**, 2121 (1982).

[5]J. P. Attfield, Solid State Sci. **8**, 861 (2006).
[6]J. P. Wright, J. P. Attfield, and P. G. Radaelli, Phys. Rev. Lett. **87**, 266401 (2001).
[7]J. P. Wright, J. P. Attfield, and P. G. Radaelli, Phys. Rev. B **66**, 214422 (2002).
[8]J. Blasco, J. Garcia, and G. Subias, Phys. Rev. B **83**, 104105 (2011).
[9]R. J. Goff, J. P. Wright, J. P. Attfield, and P. G. Radaelli, J. Phys. Condens. Matter **17**, 7633 (2005).
[10]E. Nazarenko, J. E. Lorenzo, Y. Joly, J. L. Hodeau, D. Mannix, and C. Marin, Phys. Rev. Lett. **97**, 056403 (2006).
[11]Y. Joly, J. E. Lorenzo, E. Nazarenko, J. L. Hodeau, D. Mannix, and C. Marin, Phys. Rev. B **78**, 134110 (2008).
[12]S. R. Bland, B. Detlefs, S. B. Wilkins, T. A. W. Beale, C. Mazzoli, Y. Joly, P. D. Hatton, J. E. Lorenzo, and V. A. M. Brabers, J. Phys.: Condens. Matter **21**, 485601 (2009).
[13]J. E. Lorenzo, C. Mazzoli, N. Jaouen, C. Detlefs, D. Mannix, S. Grenier, Y. Joly, and C. Marin, Phys. Rev. Lett. **101**, 226401 (2008).
[14]H. Seo, M. Ogata, and H. Fukuyama, Phys. Rev. B **65**, 085107 (2002).
[15]H. T. Jeng, G. Y. Guo, and D. J. Huang, Phys. Rev. Lett. **93**, 156403 (2004).
[16]H. T. Jeng, G. Y. Guo, and D. J. Huang, Phys. Rev. B **74**, 195115 (2006).
[17]J. van den Brink and D. I. Khomskii, J. Phys.: Condens. Matter **20**, 434217 (2008).
[18]K. Yamauchi, T. Fukushima, and S. Picozzi, Phys. Rev. B **79**, 212404 (2009).
[19]F. Zhou and G. Ceder, Phys. Rev. B **81**, 205113 (2010).
[20]T. Fukushima, K. Yamauchi, and S. Picozzi, J. Phys. Soc. Jpn. **80**, 014709 (2011).
[21]M. S. Senn, J. P. Wright, and J. P. Attfield, Nature (London) **481**, 173 (2012).
[22]P. Blaha, K. Schwarz, G. K. H. Madsen, D. Kvasnicka, and J. Luitz, *Wien2k, An Augmented Plane Wave + Local Orbitals Program for Calculating Crystal Properties* (K. Schwarz, Techn. Universität Wien, Austria, 2001).
[23]J. P. Perdew, K. Burke, and M. Ernzerhof, Phys. Rev. Lett. **77**, 3865 (1996).
[24]V. I. Anisimov, I. V. Solovyev, M. A. Korotin, M. T. Czyżyk, and G. A. Sawatzky, Phys. Rev. B **48**, 16929 (1993).
[25]L. V. Gasparov, D. B. Tanner, D. B. Romero, H. Berger, G. Margaritondo, and L. Forro, Phys. Rev. B **62**, 7939 (2000).
[26]K. Momma and F. Izumi, J. Appl. Crystallogr. **44**, 1272 (2011).
[27]P. G. Radaelli, Y. Horibe, M. J. Gutmann, H. Ishibashi, C. H. Chen, R. M. Ibberson, Y. Koyama, Y.-S. Hor, V. Kiryukhin, and S.-W. Cheong, Nature (London) **416**, 155 (2002).
[28]M. Schmidt, W. Ratcliff, P. G. Radaelli, K. Refson, N. M. Harrison, and S. W. Cheong, Phys. Rev. Lett. **92**, 056402 (2004).
[29]Y. Horibe, M. Shingu, K. Kurushima, H. Ishibashi, N. Ikeda, K. Kato, Y. Motome, N. Furukawa, S. Mori, and T. Katsufuji, Phys. Rev. Lett. **96**, 086406 (2006).